Atmospheric Pollution Research 13 (2022) 101566



Contents lists available at ScienceDirect

Atmospheric Pollution Research

journal homepage: www.elsevier.com/locate/apr

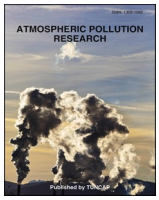



Compensatory effect of biomass burning on black carbon concentrations during COVID-19 lockdown at a high-altitude station in SW India

Subrata Mukherjee [a,b], Aastha Verma [c], Guman Singh Meena [a,*], Sandeep Kodoli [a], Pallavi Buchunde [a,b], Mohammed Yusuff Aslam [a], Rohit Dilip Patil [a], Abhilash Panicker [a], Pramod Digambar Safai [a], Govindan Pandithurai [a]

[a] Indian Institute of Tropical Meteorology, Ministry of Earth Sciences, Pune, India
[b] Savitribai Phule Pune University, India
[c] Central University of South Bihar, India

ARTICLE INFO

Keywords:
Black carbon
Source apportionment
AAE
Radiative forcing
Brown carbon

ABSTRACT

The characteristics of black carbon (BC) aerosols, their sources, and their impact on atmospheric radiative forcing were extensively studied during the COVID-19 lockdown (28th March–31st May 2020) at a high-altitude rural site over the Western Ghats in southwest India. BC concentration and the contribution of BC originating from biomass burning (BC_{bb}) estimated from the aethalometer model during the lockdown period were compared with the same periods in 2017 and 2018 and with the pre-lockdown period (1st February to March 20, 2020). BC concentrations were 44, 19, and 17% lower during the lockdown period compared with the pre-lockdown periods of 2020 and similar periods (28th March to 31st May) of 2017 and 2018, respectively. BC_{bb} contributed ~50% to total BC during the lockdown period of 2020 and compensated for the decrease in BC concentration due to lower traffic emissions. The characteristics of light-absorbing organic carbon (brown carbon; BrC) absorption at 370 nm were evaluated during the lockdown and the pre-lockdown periods of 2020, 2017, and 2018. The BrC was estimated to be the highest during the lockdown period of 2020. Finally, atmospheric radiative forcing was calculated using the mean BC concentration during the pre-lockdown, lockdown, and similar periods (28th March to 31st May) of 2017 and 2018.

Author contributions

SM conceptualized the work. MYA, RDP collected the data and performed QA/QC. SM, AV, GSM, PB and SK performed all the analysis and calculations. SM, AV, GSM wrote the paper. AP, GP, and PDS helped with the data interpretation and manuscript corrections.

1. Introduction

Atmospheric submicron aerosols play a crucial role in modulating the earth's radiation budget: i) by scattering and absorption of solar radiation (direct effect; Twomey 1977) and ii) by modulating the cloud microphysical properties and its lifetime (indirect effect). Black carbon (BC) is a carbonaceous component of aerosols and is primarily emitted from the incomplete combustion of fossil fuels and biomass burning. Although BC contributes a few percent of the total aerosol mass (Marinoni et al., 2010; Raju et al., 2016; Safai et al., 2014), it significantly modulates the earth's radiation budget with a total estimated forcing of 1.1 W/m^2, which is 65% is due to CO_2 (Bond et al., 2013). In addition, BC (coated or uncoated) can act as cloud condensation nuclei, affecting cloud formation and precipitation processes (Wang et al., 2016). Thus, a better understanding of BC aerosols and their sources, emissions, and transport mechanisms will help plan an effective mitigation strategy to prevent atmospheric warming.

BC aerosols are fine in size (<1 μm), chemically inactive, and have a short lifetime (days to a week) in ambient air conditions (Cape et al., 2012; Lund et al., 2018). Typically, anthropogenic activities are the primary source of emissions (Raju et al., 2011). However, natural sources, such as forest fires, can also contribute significantly to the observed BC. The major emitters of BC are open burning, domestic

Peer review under responsibility of Turkish National Committee for Air Pollution Research and Control.
* Corresponding author.
E-mail address: gsm@tropmet.res.in (G.S. Meena).

https://doi.org/10.1016/j.apr.2022.101566
Received 28 December 2021; Received in revised form 23 September 2022; Accepted 24 September 2022
Available online 27 September 2022
1309-1042/© 2022 Turkish National Committee for Air Pollution Research and Control. Production and hosting by Elsevier B.V. All rights reserved.

burning, and vehicular and industrial emissions (Singla et al., 2018). Globally, 60% of BC emissions are contributed by biofuels and open fires. Their contribution primarily depends on the type of biofuels used, their water content, and burning conditions (Singh et al., 2020; Reyes-Villegas et al., 2021). In rural areas, domestic burning (using dung cake, straw, husks, firewood, etc.) is a principal source of BC and is a primary cause of indoor pollution (Janssen et al., 2012).

Sandradewi et al. (2008) proposed a model that utilizes the differential wavelength-dependent absorption of BC and absorbing organic carbon (to segregate light absorption due to brown carbon (BrC) from BC) to estimate the BC contribution from biomass burning and traffic, respectively. Dumka et al. (2018) have estimated the biomass burning contribution as ~28% of the total observed BC over a mega city like Delhi. The extent of biomass burning varies from 6 to 27% over the Indian subcontinent, along with the heterogeneity in their emission sources (Ahmedabad: Rajesh and Ramachandran 2022, Pune and Mahabaleshwar: Meena et al., 2021). Srivastava et al. (2011) reported that BC induces great uncertainty in constraining aerosol radiative forcing. Thus, a better understanding of its sources and atmospheric abundance is crucial for reducing the uncertainties associated with radiative forcing (Wang et al., 2016).

It is well known that BC and dust are primary contributors to aerosol absorption. However, a fraction of organic carbon termed BrC showed strong light-absorption efficiency similar to that of BC (Andreae et al., 2006; Formenti et al., 2003; Kirchstetter et al., 2004; Lack et al., 2013; Wang et al., 2018), which may modulate the Earth's radiation budget. BrC has a strong light absorbing tendency near the UV to visible range (300–550 nm) (Formenti et al., 2003; Kirchstetter et al., 2004). BrC can be added to the atmosphere from the incomplete combustion of biofuels and the oxidation of volatile organic compounds (VOCs), leading to secondary organic aerosol (SOA) formation (Chen and Bond, 2010; Lack et al., 2012; Saleh et al., 2014; Laskin et al., 2015; Healy et al., 2015). Wang et al. (2018) attempted to estimate the absorption coefficient of BrC by utilizing the black carbon absorption properties (as measured by a multi-wavelength aethalometer and single-particle soot photometer) over the Yangtze River Delta (YRD), China. The BrC was estimated to contribute 10–24% of total absorption at 370 nm as measured by a multi-wavelength aethalometer. Feng et al. (2013) reported that global radiative forcing due to BrC is almost one-quarter that of BC. Thus, a detailed study of BC and BrC characteristics is crucial.

To control the spread of the COVID-19 pandemic in India, a nationwide lockdown was implemented in different phases from 25th March to May 31st, 2020, resulting in a low emission of anthropogenic pollutants. Due to the lockdown, a significant decrease in vehicular movement, construction and industrial work, and other commercial activities was observed across the country, reducing PM_1, $PM_{2.5}$, and PM_{10} concentrations. Many studies have discovered that the implementation of lockdown in India and other parts of the world has resulted in a significant reduction in BC and other pollutant mass concentrations (Ajay et al., 2021; Goel et al., 2021; Jafar and Harrison, 2020; Manohar et al., 2021; Milinković et al., 2021; Palle et al., 2021; Rajesh and Ramachandran 2022; Rathod et al., 2021; Shen et al., 2021). Conversely, recent studies over the Indian subcontinent using satellite data (Ratnam et al., 2021; Bhawar et al., 2021; Pandey and Vinoj, 2021) revealed that the central Indian region showed an increasing trend in aerosol optical depth (AOD) during the lockdown period, although there was a decrease over the Indo-Gangetic Plain (IGP) region and other parts of India. This study highlights the diurnal changes in BC concentration, absorption Ångström exponent (AAE) value, and BC from fossil fuel (BC_{ff}) and biomass burning (BC_{bb}) concentrations during the pre-lockdown (1st February to March 20, 2020) and lockdown (28th March to May 31, 2020) periods over Mahabaleshwar (17.92° N, 73.65° E). Furthermore, the lockdown time of BC and its associated properties were compared with those of previous years (2017 and 2018) to evaluate the extent of lockdown effects on atmospheric BC abundance. Finally, an effort was made to quantify the changes in BC atmospheric radiative forcing due to lockdown and the possible contribution of BrC at 370 nm wavelength. This study is expected to contribute to the global data pool of BC, which is crucial for validating and estimating the uncertainties associated with model estimations of aerosol-related radiative forcing.

2. Site description and methodology

The observational site, High Altitude Cloud Physics Laboratory (HACPL) Mahabaleshwar (17.92° N, 73.65° E), is situated 1378 m above mean sea level in the Western Ghats mountainous region in southwest India. The site is surrounded by dense forests in all directions. There is a market and village near the observatory (to its south of the observatory), which can be considered as point sources for local emissions. Since Mahabaleshwar is a famous tourist spot, the site is also surrounded by several hotels. The site was influenced by different types of air masses throughout the year. The polluted continental air mass (from northwest to northeast) dominates the site during the post-monsoon (October–November) and winter period (December–February) (Mukherjee et al., 2018; Mukherjee et al., 2020; Meena et al., 2021; Buchunde et al., 2022). Cleaner maritime air masses prevail during the pre-monsoon (March–May) and monsoon (June–September) periods (Singla et al., 2018; Meena et al., 2021; Buchunde et al., 2022). The site also receives very high rainfall (~5500 mm) during monsoon. This study primarily utilized data from February to May 2020. The observational datasets were divided into two periods: pre-lockdown (1st February to March 20, 2020) and lockdown (28th March to May 31, 2020). We also utilized BC data from 28th March to May 31, 2017 and 2018 for the comparative study. The average meteorological parameters for these periods are listed in Table S1. The meteorological parameters (Table S1) did not vary much from 28th March to May 31, 2020, compared with 2017 and 2018.

A seven-wavelength dual-spot aethalometer (Magee Sci. Inc. USA, Model AE-33; Drinovec et al., 2015) was used to measure the BC concentration. A 2.5 μm cut-off cyclone was used in the Aethalometer sampling inlet line for BC measurement. The aethalometer measures the optical attenuation of light passed through the aerosol-laden filter to determine the concentration of BC aerosol expressed in terms of nanograms of BC per cubic meter. This attenuation by the sampled aerosols was proportional to the deposited absorbing BC aerosols. Thus, the BC mass concentration is given by the rate of change in the optical attenuation. The aethalometer records the attenuation coefficient at seven wavelengths, including 370, 470, 520, 590, 660, 880, and 950 nm, covering near-UV to the near-IR range. The data were collected with a time resolution of 1 min and a minimum detection limit of 0.1 $\mu g/m^3$ (Hansen et al., 1984; Hansen, 2007). Corrections of filter-based measurements, which modulate the effective optical path length, were considered for the AE-33 data. The data were corrected for multiple scattering through aerosol particles and filter paper (Collaud et al., 2010; Drinovec et al., 2015). The correction related to the filter paper loading effect was performed in AE-33, following Virkkula et al. (2007). This correction applies a compensation factor in $(1 + k \times ATN)$, where k is calculated for each filter change, and ATN corresponds to the attenuation. This algorithm was used to design the dual-spot technology aethalometer (model AE33) that intrinsically compensates for filter-loading effects using a two-beam system with different flow rates (Drinovec et al., 2015). The C value of the Pallflex Teflon-coated glass fiber (TFE; Part No. M8060) filter tape was set to 1.57 (manufacturer recommended value) in AE33 software and was not wavelength-dependent (Drinovec et al., 2015).

The absorption coefficients derived from the aethalometer were used to estimate the contribution of BC_{ff} and BC_{bb} to the total BC concentrations using the aethalometer model (Sandradewi et al., 2008). Wavelengths of 470 and 880 nm were used to quantify the contribution of BC_{ff} and BC_{bb} to the total observed BC (Crippa et al., 2013; Meena et al., 2021). More details regarding the model can be found in previous

studies (Sandradewi et al., 2008; Crippa et al., 2013; Meena et al., 2021). AAE values of 1.75 and 1 for biomass burning and fossil fuel emissions, respectively (Meena et al., 2021), were utilized to evaluate the contribution of biomass burning and traffic emissions. The uncertainty related to the assumed AAE values was also evaluated through a sensitivity test by changing the AAE value by 10% (Meena et al., 2021). Fig. S1 represents the time series of the BC_{bb} (S1. a) and BC_{ff} (S1. b), calculated using an AAE value of 1.75 along with the standard deviation (evaluated by assuming different AAE values for BC_{bb}). The vertical red line indicates the start of the lockdown. The results revealed that the aethalometer model was more sensitive to lower AAE_{bb} values considered in estimating BC_{bb} (1.575; 10% change of 1.75). An average of 23% change in the estimated BC_{bb} contribution was observed. In contrast, a higher AAE value ($AAE_{bb} = 1.925$) induced less variability in the BC_{bb} contribution. Mukherjee et al. (2021) estimated the AAE value of wood-burning emissions to be 1.7–1.8 through chamber experiment. Thus, the assumption of an AAE value of 1.75 for BC_{bb} was expected to be associated with minimal errors. Notably, the biomass burning-related AAE varies widely (1.2–2.9) (Kirchstetter et al., 2004; Hoffer et al., 2006; Lewis et al., 2008; Sandradewi et al., 2008; Chakrabarty et al., 2010; Lack and Langridge, 2013; Shen et al., 2017) and may add non-negligible uncertainties in the estimated BC_{bb} contribution.

The sub-micron aerosol chemical composition data were obtained by the time-of-flight aerosol chemical speciation monitor (TOF-ACSM) in 2017 and 2018 and by a high-resolution time-of-flight aerosol mass spectrometer (HR-TOF AMS) in 2020. The details of the operation, calibration, maintenance, and data correction are provided elsewhere (Aiken et al., 2008; Ng et al., 2011; Mukherjee et al., 2018; Mukherjee et al., 2021). Organic data obtained from TOF-ACSM and HR-TOF AMS were primarily used for this study.

Delta-C (BC_{370nm}-BC_{880nm}) is the difference between BC_{370nm} and BC_{880nm} and serves as an indicator for the wood combustion particles. Biomass-burning particles show better absorbance at 370 than at 880 nm. Delta-C provides an enhanced absorption value by subtracting the measured BC concentration at 370 nm from that of BC at 880 nm, as mentioned in Wang et al.

To estimate atmospheric BC radiative forcing, we followed the methodology described by Panicker et al. (2010, 2013). The observed BC concentration over the region was converted to an equivalent number density as described by Hess et al. (1998). The optical properties of aerosols and clouds (OPAC) software packages were then used to convert the BC number density to BC optical properties (Hess et al., 1998). The OPAC output consists of aerosol optical depth (AOD), single scattering albedo (SSA), asymmetry parameter (ASP), and Ångström exponent (AE). A continental averaging scheme was chosen in the OPAC model to match the measurement location. The output provided by the OPAC model was subsequently fed into the Santa Barbara DISORT Atmospheric Radiative Transfer (SBDART) to estimate the radiative forcing of BC aerosols (Ricchiazzi et al., 1998). Apart from the optical properties as input, columnar data on ozone (obtained from the ozone monitoring instrument, such as OMI aboard NASA's Aura satellite) and water vapor (obtained from the Moderate Resolution Imaging Spectroradiometer, such as MODIS onboard NASA's Terra and Aqua satellites) were used in the model for better accuracy. The default vertical profiles for the meteorological variables for the tropics were used in the calculations. SBDART has the option of switching the aerosol interactions on/off in the model. Hence, the model was run with and without aerosols. The net radiation difference between the simulations was estimated. BC radiative forcing at the surface, top of the atmosphere, and the atmosphere was then evaluated using the SBDART output data.

The BrC characteristics at a near-UV wavelength (370 nm) were estimated following Wang et al. (2018). The BrC absorption at 370 nm can be calculated as follows:

$$b^{370}_{abs_BC} = b^{880}_{abs} \times (880/520)^{AAE^{520-880}_{BC}} \times (520/370)^{AAE^{370-520}_{BC}} \quad (1)$$

$$b_{abs_BrC} = b^{370}_{abs} - b^{370}_{abs_BC} \quad (2)$$

where b^{880}_{abs} and b^{370}_{abs} is the absorption coefficients at 880 and 370 nm, respectively. $AAE^{520-880}_{BC}$ and $AAE^{370-520}_{BC}$ are the absorption Ångström exponents estimated for pure BC (fossil fuel emission) at 520–880 nm and 370–520 nm. This AAE segregation-based method is widely utilized for estimating the BrC absorption coefficient (Lack and Langride, 2013; Mohr et al., 2013; Wang et al., 2018). The wavelength dependence of pure BC is considered to be 1, but it varies widely owing to the underlying factors (Lack and Cappa., 2010; Bond et al., 2013; Wang et al., 2018). In this study, pure BC absorption characteristics of pure BC at different wavelength ranges were evaluated using a fullerene solution (in water). Fullerene is widely used as a standard for calibration of instruments related to BC concentration and associated optical properties (such as SP2) (Schwarz et al., 2006; Schwarz et al., 2010; Gysel et al., 2011). The fullerene solution was passed through an atomizer and a diffusion dryer (for drying aerosols) before reaching the aethalometer inlet. The entire assembly was checked for leaks by zero particle count in a condensation particle counter (CPC) when the atomizer was off. The AAE values for the 520–880 nm and 370–520 nm wavelength ranges were estimated to be 1.21 and 0.98, respectively. These values were utilized in equation (i) to predict the absorption characteristics of BC at 370 nm ($b^{370}_{abs_BC}$). The obtained $b^{370}_{abs_BC}$ was then subtracted from the total absorption at 370 nm to determine the extent of BrC absorption.

3. Results and discussions

3.1. BC mass concentration

Fig. 1 shows the diurnal variation of the mean BC mass concentration at 880 nm during the pre-lockdown (1st February to March 20, 2020) and lockdown (28th March to May 31, 2020) periods. The vertical line represents the standard deviations. As depicted in the figure, the BC concentration (BC_{880}) decreased during the lockdown period compared with the pre-lockdown period. During the pre-lockdown period, the average diurnal BC exhibited two prominent peaks, one in the morning (7:00–10:00 a.m.) and the other in the evening (6:00–10:00 p.m.). Both peaks also existed during the lockdown period but were much smaller and less intensive than those in the pre-lockdown period. The observed morning and evening high BC concentrations during the pre-lockdown period can be attributed to the emissions from certain combustion activities. In addition to traffic emissions, biomass burning emissions from indoor and/or outdoor sources are expected to contribute to the

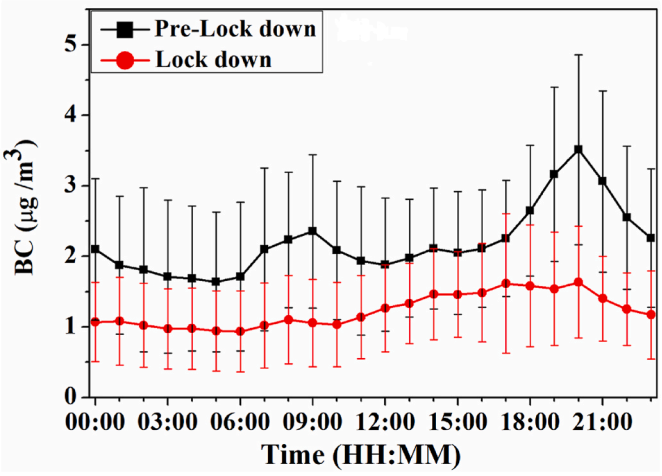

Fig. 1. Diurnal variation of BC concentration at 880 nm as observed during pre-lockdown 2020 (1st February to 20th March) and lockdown 2020 (28th March to 31st May) at HACPL, Mahabaleshwar.

observed BC (Kodandapani, 2013; Meena et al., 2021). The BC mass concentrations observed at 880 nm during the pre-lockdown and the lockdown periods ranged from 1.64 to 3.51 μg/m^3 and 0.93–1.63 μg/m^3, with a mean value of 2.20 ± 1.12 μg/m^3 and 1.23 ± 0.68 μg/m^3 (Table S2), respectively. The significant reductions in BC concentration (~44%) recorded during the lockdown period compared with pre-lockdown may be attributed to the reduction of emissions from industries and vehicular traffic during the lockdown period. The impact of biomass burning emissions on BC concentrations during the lockdown period is presented in Section 3.3.

The BC mass concentrations at different locations in India were compared and are presented in Table 1. As shown in Table 1, the highest reduction in BC mass concentration was observed for megacities (urban locations), such as Delhi (78%; Goel et al., 2021) and Bengaluru (60%; Ajay et al., 2021). Rural and semi-arid regions tended to show a lesser reduction in BC mass concentration due to lockdown (Anantapur: Palle et al., 2021; Ahmedabad: Rajesh and Ramachandran, 2022). A possible reason could be that the BC mass concentrations in urban locations were mainly driven by the extent of fossil fuel emissions, which were minimal during the lockdown. Notably, the pre-lockdown period considered here is from winter to the beginning of the pre-monsoon (summer) period, when the prevailing air mass is dominant of inland origin. The air mass during the lockdown period was dominated by maritime origin, indicating a lower contribution from transported BC (Mukherjee et al., 2018). However, more detailed studies are required to ascertain the contribution of different sources to the observed BC. To corroborate the variation in BC, sub-micron organic aerosol data obtained from HR-TOF AMS were also utilized to study the effect of lockdown on the mass loading and variability of other aerosol components. The organics concentration (which contributes >50% of total non-refractory particulate mass ≤1 μm size (NR-PM1) mass concentration) was observed to be less during the lockdown period (3.67 ± 2.71 μg/m^3) compared with the pre-lockdown period (5.84 ± 2.55 μg/m^3) of 2020. The sulfate concentration also showed a similar range of variation. Therefore, the decrease in aerosol mass concentration can be attributed to i) restricted anthropogenic activities and ii) changes in emission patterns from the winter to the pre-monsoon season. To understand the changes in emission patterns from the pre-lockdown period to the lockdown period, the mass spectrum was evaluated and plotted during the pre-lockdown and lockdown periods in 2020 (Fig. S2). As depicted in the figure, there was a drastic change in the organic mass spectrum. The fractions of m/z 41, 43, 55, 57 (f_{41}, f_{43}, f_{55}, f_{57}), which represent the extent of fossil fuel emissions (traffic or combustion), decreased during the lockdown period when compared with the pre-lockdown period. There was a noticeable increase in the fraction of m/z44 (f_{44} highest), m/z 60 (f_{60}), and m/z 73 (f_{73}). m/z 60 and m/z 73 are widely considered important tracers for biomass burning (fragments of levoglucosan), as reported earlier (Alfarra et al., 2007; Crippa et al., 20013; Mukherjee et al., 2018). Therefore, the organic aerosol mass spectrum indicated an enhancement of the biomass burning contribution during the lockdown period of 2020.

3.2. Absorption ångström exponent and delta C

The absorption Ångström exponent (AAE) is widely used as an essential aerosol optical parameter to indicate the influence of different sources on the observed BC concentration. The AAE has a specific value for each source type. If the AAE of BC is close to 1.0 (0.9–1.1; Sandradewi et al., 2008), BC is considered to be emitted from fossil fuel combustion. A higher AAE value corresponds to the biomass burning emitted by BC (Kirchstetter et al., 2004; Hoffer et al., 2006; Sandradewi et al., 2008; Russell et al., 2010). In this study, the calculated AAE value during the pre-lockdown (1.25 ± 0.17) was lower than that during the lockdown period (1.46 ± 0.13). The average AAE diurnal varied from 1.18 to 1.36. During the pre-lockdown period, the lockdown variation ranged from 1.39 to 1.56 (Fig. 2). The AAE increased in the morning (06:00 h to 09:00 h) and evening (21.00 h) during the pre-lockdown periods. The AAE values during the lockdown were evaluated to be higher (than those during the pre-lockdown period) throughout the day, with a peak in the morning and evening hours indicating active biomass burning sources throughout the day. As shown in Fig. 2, the extent of BC emissions from combustion-related traffic sources decreased significantly from the pre-lockdown to the lockdown period.

In addition to AAE, the delta-C value was also utilized to quantify the impact of biomass burning over the observational site. Delta-C was calculated as the difference between the observed mass concentrations of BC at 370 and 880 nm (Wang et al., 2011; Singla et al., 2018; Meena et al., 2021). Delta-C was previously used as a tracer for biomass burning (Wang et al., 2012; Singla et al., 2018). As shown in Fig. 2b, the estimated delta-C consisted of morning and early night hour peaks, with a higher peak during the afternoon hours of the pre-lockdown period. The study site is a famous tourist site. Cooking and water-heating activities (using wood pallets) were prominent during the pre-lockdown period. These signature peaks were absent during the lockdown period. Delta-C gradually increased from morning to late evening, with a peak at approximately 20:00, indicating the presence of indoor/outdoor burning activities throughout the day. In addition, the reduced impact of these activities due to the closing of hotels and restaurants during the lockdown compared with the pre-lockdown period significantly modified the delta-C variation. It is also important to note that delta-C may indirectly indicate the abundance of light-absorbing organic carbon, which may be emitted from biomass burning or formed by photochemical aging processes. Harrison et al. (2013) highlighted the uncertainties and pointed out the drawbacks of relying on delta-C to infer the wood smoke. However, a comparison of diurnal variation of the fraction of m/z 60 (f_{60}; a tracer of Levoglucosan emitted during biomass burning; Alfarra et al., 2007; Crippa et al., 2013; Mukherjee et al., 2018) with delta-C indicated that delta-C was able to replicate diurnal biomass burning emissions (Fig. S3). Wang et al. (2012) have shown that >72% of the delta-C was associated with the wood-burning factor through

Table 1
The comparison of BC mass concentration before and after lockdown period at different locations in India.

Location	Altitude	Type of site	BC Concentration (μg/m^3)				References
			Lockdown period	Lockdown Concen.	Pre-Lockdown Concen.	Changes in %	
HACPL, Mahabaleshwar	1378 m	Rural	28th March to May 31, 2020	1.23 ± 0.68	2.20 ± 1.12	44% reduction	Present study
Delhi	216 m	Urban	25th March to April 14, 2020	1.73	7.93	78% reduction	Goel et al. (2021)
Bengaluru	920 m	Urban	24th March to April 14, 2020	1.69 ± 0.04	4.33 ± 0.15	60% reduction	Ajay et al. (2021)
Ahmedabad	55 m	Semi-arid	25th March to May 31, 2020	2.2 ± 0.7	3.5 ± 1.3	35% reduction	Rajesh and Ramachandran (2022)
Anantapur	335m	Semi-arid	25th March to 30th June 2020	1.11 ± 0.14	1.74 ± 0.36	35% reduction	Palle et al. (2021)

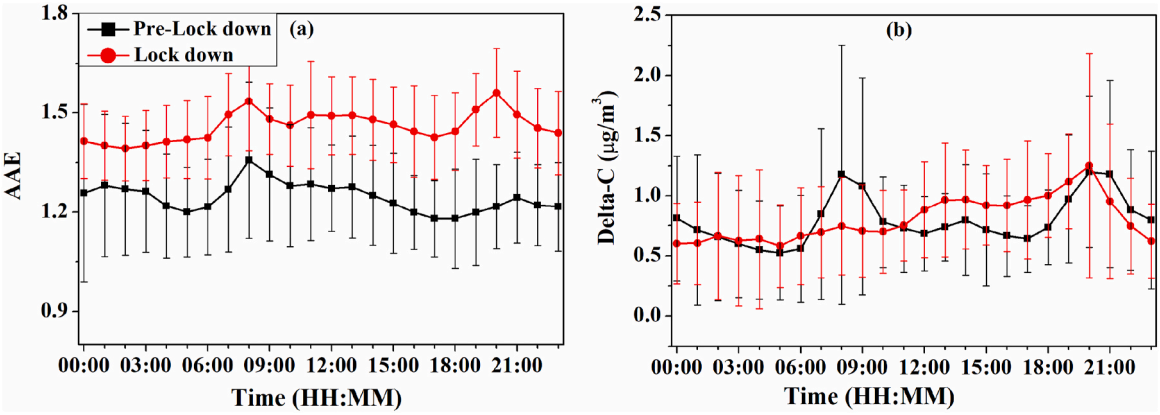

Fig. 2. Diurnal variation of AAE (mass absorption cross section values 18.47 m^2/g for 370 nm and 7.77 m^2/g for 880 nm) (a) and Delta-C (estimated as difference in BC mass concentration at 370 nm and 880 nm) (b) as observed during Pre-Lockdown 2020 (1st February to 20th March) and lockdown period 2020 (28th March to 31st May) at HACPL, Mahabaleshwar.

positive matrix factorization (PMF) analysis. Therefore, delta-C can be utilized as a good indicator of biomass burning in this study.

3.3. Source apportionment of BC

In addition to estimating delta-C and AAE, source apportionment of BC (BC_{bb} and BC_{ff}) was performed during pre-lockdown and lockdown, utilizing the wavelength dependency of BC (details given in Crippa et al., 2013; Meena et al., 2021). The estimated diurnal trends of BC_{bb} and BC_{ff} during the pre-lockdown and lockdown periods are shown in Fig. 3. During the pre-lockdown period, the diurnal profile of BC_{bb} concentrations had a multi-modal feature with characteristic peaks during the morning, afternoon, and evening. The fossil fuel emissions were higher throughout the day and reached a maximum during the late evening hours (2.99 $\mu g/m^3$ at 20:00 h). The average ratio of traffic to biomass burning contribution was estimated to be 4.11, which indicates the dominance of traffic emissions on the observed BC during the pre-lockdown period.

During the lockdown period, the mean mass concentrations of BC_{bb} and BC_{ff} were 0.61 ± 0.46 $\mu g/m^3$ and 0.62 ± 0.44 $\mu g/m^3$, respectively, which indicated that the fossil fuel contribution reduced drastically due to lockdown restrictions. There was an appreciable increase in the BC_{bb}

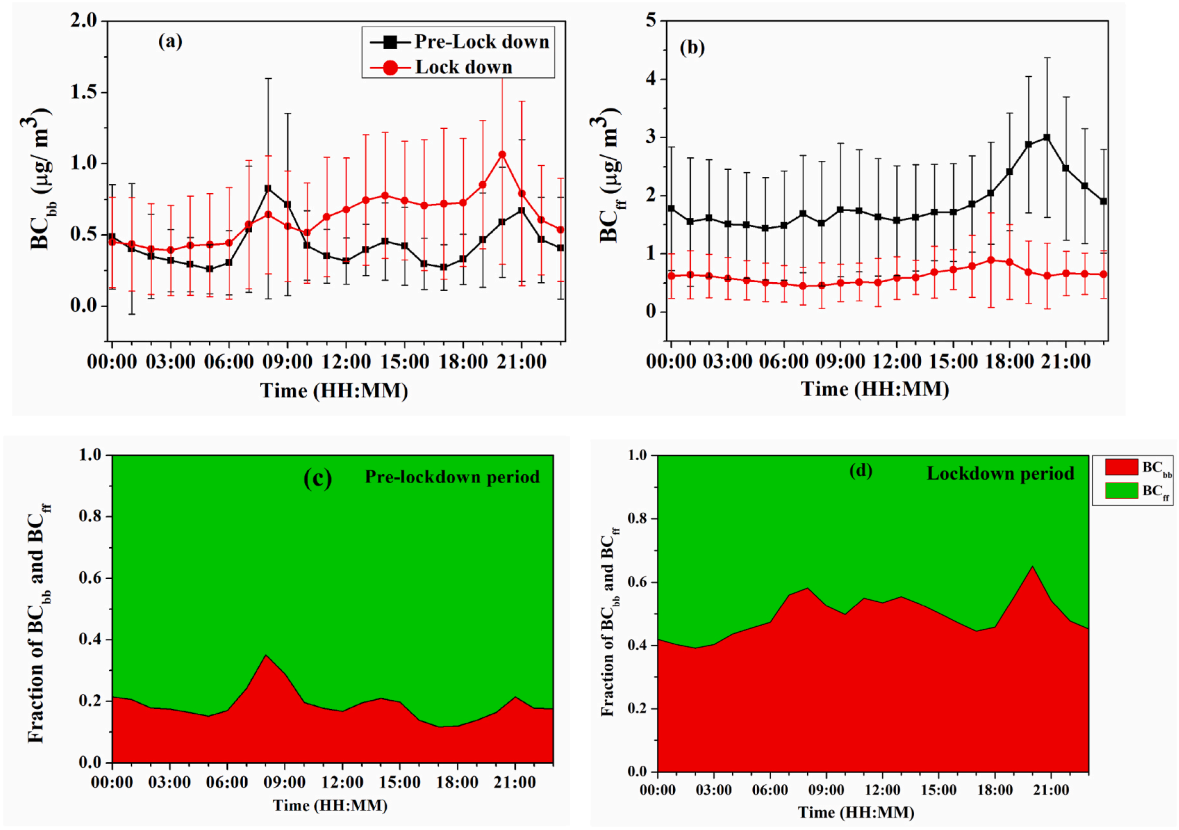

Fig. 3. Mean diurnal variation of **BC_{bb}** (a), and **BC_{ff}** (b) as a function of time during the study period Pre-Lockdown 2020 (1st February to 20th March) and lockdown 2020 (28th March to 31st May) at Mahabaleshwar. Fig. (c) and (d) represents the fraction of contribution of BC_{bb} and BC_{ff} during pre-lockdown and lockdown period respectively.

concentration during the lockdown period (Fig. 3d). The BC_{bb} concentration was high throughout the day, peaking at 1.06 μg/m^3 during the evening (20:00 h). The estimated contribution of BC_{bb} to total BC was high throughout the day, with a maximum of ~65% during the evening hours (Fig. 3d). On average, BC_{ff} contributed about 50% of the total observed BC during the lockdown period. The BC_{bb} and BC_{ff} contributions to total BC were 20 and 81%, respectively, during the pre-lockdown period (Fig. 3c). Therefore, BC_{bb} concentration increased (~42%) during the lockdown period and BC_{ff} concentration decreased significantly (~65%) compared with the pre-lockdown period. The fraction of m/z 60 data (f_{60}) obtained from AMS was further compared with that of BC_{bb} (Fig. S4). As depicted in Fig. S4, the diurnal variation of f_{60} was similar to that of BC_{bb} estimated using the aethalometer model.

3.4. Comparison with previous year's observations

The comparison of BC concentration and its source characteristics during the pre-lockdown and lockdown periods covers two seasons: winter to pre-monsoon (1st February to March 20, 2020; pre-lockdown) and pre-monsoon season (28th March to May 31, 2020; lockdown). There was inherent heterogeneity due to changes in the prevailing air masses during these two seasons. The significant reduction observed in the BC concentrations due to the decrease in anthropogenic emissions during the lockdown restrictions (65% reduction in BC_{ff}) may be a result of changes in air mass and the source pattern due to the transition from winter to the pre-monsoon season. Hence, comparisons of BC mass concentration and its source contribution during similar periods of previous years (28th March to May 31, 2017, and 2018) with that of 2020 were evaluated. Statistically significant BC data for 2019 were not available due to technical problems. BC concentrations at both 370 and 880 nm were high in the pre-lockdown period of 2020, which was also higher than those observed in 2017 and 2018 (Fig. 4a and b, S5 and S6). The BC characteristics were similar during the pre-lockdown period of 2020 and a similar period of 2018, except that the BC_{bb} contribution was slightly higher during 2018. The estimated AAE value (Fig. 4c; Table S2) was higher during the lockdown period of 2020 than in 2017 and 2018. Delta-C (Fig. 4d, S5, and S6; Table S2) also showed a higher value during the lockdown period in 2020 than in 2017 and 2018. Furthermore, the derived BC_{bb} and BC_{ff} values in 2017 and 2018 were compared with the lockdown period to investigate the possible reason for the enhanced AAE (Fig. 4e and f). BC_{ff} decreased substantially (43–51%) in the lockdown period compared with 2017 and 2018. The decrease in BC_{ff} indicated that the sources contributing to BC_{ff} diminished drastically during 2020 compared to those in 2017 and 2018. Whereas, BC_{bb} contribution to total BC increased significantly during the lockdown period of 2020 (50%) compared with the similar period of 2017 (17%). These estimates indicated a significant enhancement in the contribution of biomass burning to BC, which compensated for the reduction in BC due to a large decrease in traffic emissions. We also compared the average diurnal variation of BC during the pre-lockdown period of 2018 (BC data for a similar period in 2017 were unavailable) and 2020 (Fig. S7). As shown in Fig. S7, there was a significant difference between the BC mass concentrations observed at 880 nm during the pre-lockdown period. The mean concentration of BC at 880 nm was observed to be 2.48 μg/m^3 (2018) and 2.20 μg/m^3 (2020), respectively during the pre-lockdown period (11% reduction in 2020). Although BC_{ff} was estimated to exhibit similar diurnal variability, there was a noticeable difference in the BC_{bb} variability. High concentrations were observed in the morning during the pre-lockdown period of 2020, whereas high concentrations were observed in the evening during a similar period in 2018. Interestingly, BC_{ff} substantially contributed to the observed BC during the pre-lockdown period of 2018 and 2020 (77–83%).

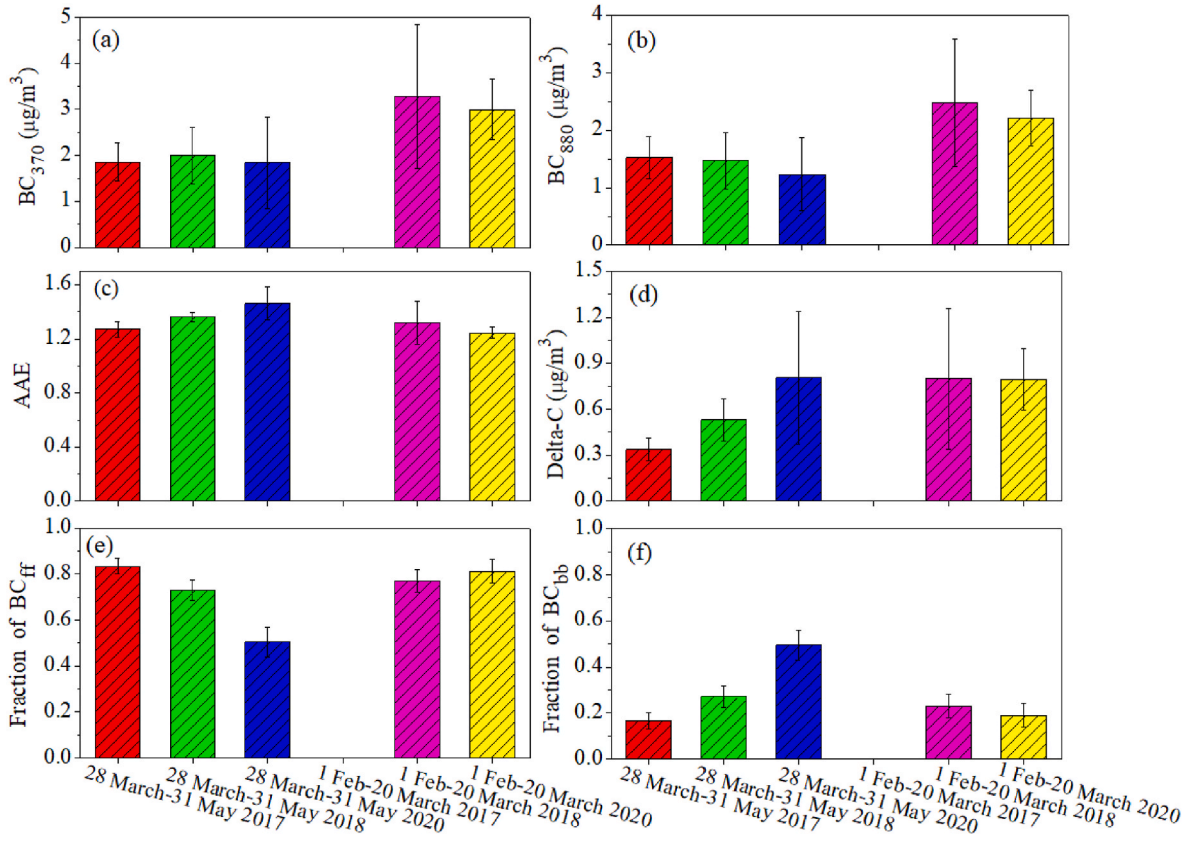

Fig. 4. BC mass concentration at 370 nm (a), 880 nm (b), AAE (c), Delta-C (d), fraction of BC_{ff} (e), and Fraction of BC_{bb} (f) during 28th March to 31st May of 2017, 2018, 2020 and 1st February to 20th March of 2017 (data not available), 2018 and 2020 at HACPL, Mahabaleshwar. The lockdown period was 28th March to 31st May 2020.

Sub-micron organic aerosol data obtained from HR-TOF AMS (during 2020) and TOF-ACSM (during the pre-lockdown and lockdown periods of 2017 and 2018) were compared to evaluate the effect of lockdown on mass loading and variability of other aerosol components. Figs. S8a and b show the mean mass concentrations of organics and sulfate during the pre-lockdown (a) and lockdown (b) periods from 2017 to 2020. The comparison between the mean organic mass concentrations during the pre-lockdown and lockdown periods of 2017, 2018, and 2020 revealed a decreasing trend. The diurnal variation in organics during the pre-lockdown (S8c) and lockdown (S8d) periods exhibited similar behavior to that of 2017, 2018, and 2020. The percentage decrease in organic mass concentration from the pre-lockdown to lockdown period was highest (37%) during 2020 compared with similar periods in 2017 (33%) and 2018 (31%). In addition, the percentage fraction of each species was estimated during the pre-lockdown and lockdown periods in 2017, 2018, and 2020. The fraction contribution of organics exhibited a decreasing trend from the pre-lockdown to the lockdown period of 2017 (0.61–0.50) and 2018 (0.68–0.60). Notably, the trend was reversed in 2020. The fraction of organics increased from 0.54 to 0.57. The increase in biomass burning emissions could be one of the reasons for the enhancement of organic fractions during the lockdown period (Fig. S2). Therefore, it can be concluded that the change in the emission pattern due to the lockdown (in 2020) influenced the aerosol mass concentration and the associated seasonal changes (winter to summer).

3.5. Radiative forcing due to BC

Atmospheric radiative forcing due to BC was estimated utilizing OPAC-derived optical parameters fed into the SBDART model. BC radiative forcing was calculated for every month from February to May 2020 using the monthly mean BC concentration (Fig. 5a). As observed from this figure, the largest atmospheric radiative forcing of BC was observed during February (13.12 W/m^2), which gradually decreased and was lowest in May 2020 (9.23 W/m^2). The difference in radiative forcing due to BC during the pre-lockdown to lockdown period was estimated to be 2.81 W/m^2 (21% decrease). The reduction in radiative forcing can be linked to the reduced emission of BC into the atmosphere. BC radiative forcing during the pre-monsoon season (March–May) of 2017 and 2018 (Fig. 5b) was further compared with BC radiative forcing during the lockdown period of 2020. Compared with the 2020 lockdown period, atmospheric radiative forcing was estimated to be about 8% higher in 2017 and 2018 (atmospheric radiative forcing 11.13 W/m^2 during 2017 and 11.11 W/m^2 during 2018) as compared with that in the 2020 lockdown period. The reduction in radiative forcing can be linked to the decrease in fossil fuel emissions due to the lockdown. The lowering of fossil fuel emissions (43–51%, compared with 2017 and 2018) was compensated by the biomass burning (which increased 61–155% compared with 2017 and 2018) emissions, resulting in minimal change in atmospheric radiative forcing. Recent studies (Ratnam et al., 2021; Pandey and Vinoj, 2021) have highlighted the impact of biomass burning, compensating for the effect of lockdown, particularly over the central Indian region. To visualize the impact of biomass burning on BC concentration during the COVID-19 lockdown period, MODIS fire count data (https://earthdata.nasa.gov/earth-observation-data/near-real-time/firms/active-fire-data) were extracted and are shown in Fig. 6 during the pre-lockdown (Fig. 6a) and lockdown (Fig. 6b) periods. The active fire counts were higher over Central India, including Gujarat, and around the observational site at Mahabaleshwar during the lockdown period than during the pre-lockdown period. Cluster analysis (Petit et al., 2017; Fig. S9) utilizing two days back trajectory data derived from HYSPLIT (Draxler and Rolph 2003) revealed that the air mass (~48% of back trajectories) was passing over/close to Gujarat and Mumbai before reaching to the observational site during the lockdown period. Satellite-derived carbon monoxide (CO) estimations showed an increase over Gujarat during the lockdown period (Fig. S10), which was not visible during similar periods in 2017 and 2018. These results indicate the regional transport of BC (emitted from biomass burning) and local emissions (domestic and/or agricultural activities), which contribute significantly to the observed BC mass concentration. It is also important to note that BrC may also contribute to atmospheric radiative forcing during the lockdown period of 2020 in addition to BC, as biomass burning significantly contributed to maintaining the atmospheric BC concentration throughout the lockdown period. However, the estimation of the radiative forcing of BrC is beyond the scope of this study. In the future, an attempt will be made to quantify the radiative forcing due to BrC.

3.6. Insight into BrC absorption

Along with BC, quantifying BrC is essential to reduce the uncertainties of aerosol-radiation interaction (ARI). Therefore, we attempted to estimate the extent of BrC absorption at near-UV wavelengths (370 nm). BrC absorption was estimated to be 9.68 Mm^{-1}, which is ~18% of the total absorption at 370 nm during the pre-lockdown period of 2020. However, BrC absorption was 8.77 Mm^{-1} which was ~26% of the total absorption (at 370 nm) during the lockdown period of 2020. Wang et al. (2018) reported that the contribution of BrC absorption to total aerosol absorption at 370 nm varied from 10 to 24% (biomass burning dominated season), with an annual average of 6.30 Mm^{-1}. Notably, BrC can be contributed by i) incomplete combustion of biomass burning and ii) oxidation of VOCs leading to SOA formation (light-absorbing type). These results also indicate the importance of BrC absorption during the lockdown. Furthermore, the BrC absorption was estimated for a similar period (28th March to 31st May) in 2017 and

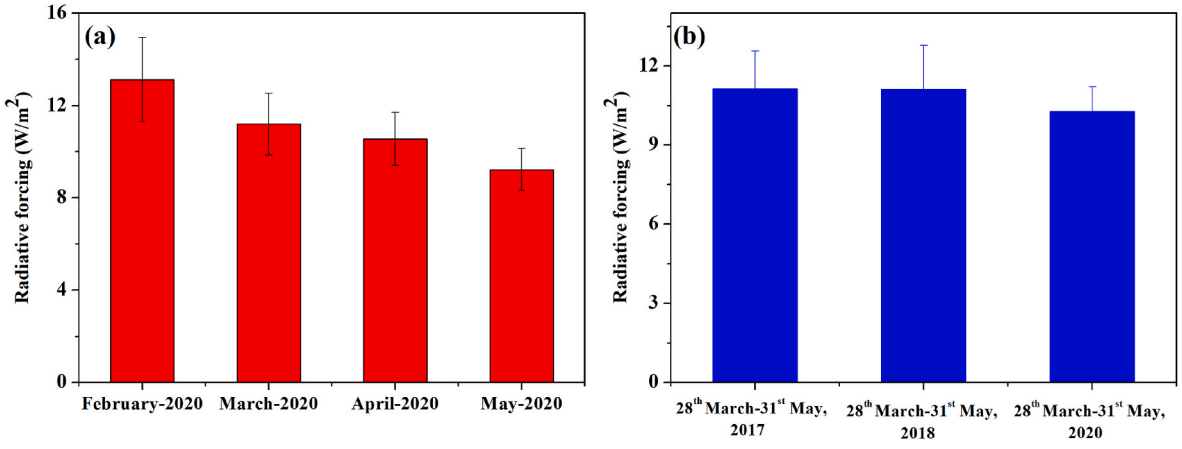

Fig. 5. Radiative forcing of Black carbon over HACPL, Mahabaleshwar month-wise (a) during 2020 and 28th March to 31st May of 2017, 2018, and 2020 (b).

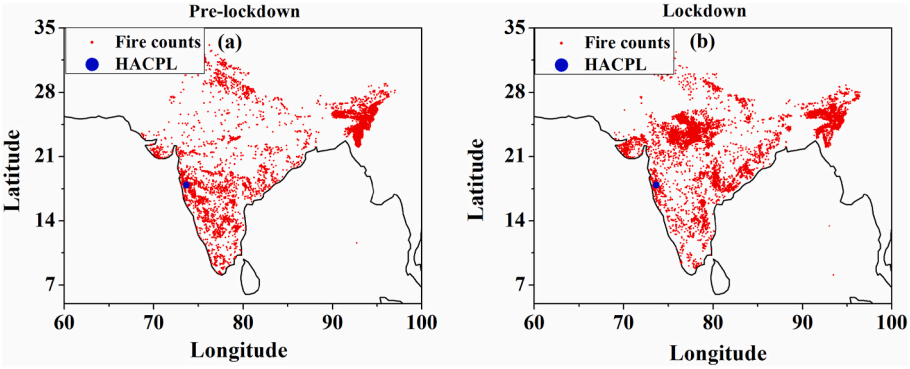

Fig. 6. Spatial map of fire counts observed over India during pre-lockdown (a) and lockdown (b) period. The blue point represents HACPL, Mahabaleshwar.

2018. The BrC absorption was 3.12 Mm^{-1} (9% of 370 nm absorption) and 6.25 Mm^{-1} (16% of 370 nm absorption) during 2017 and 2018. The extent of photochemical activity to form BrC is expected to be similar in 2017, 2018, and 2020. Whereas, the traffic contribution is expected to be low from 28th March to May 31, 2020, due to the lockdown restrictions. Therefore, the enhanced BrC absorption during the 2020 lockdown may be primarily attributed to biomass burning emissions.

4. Conclusions

The impact of COVID-19 lockdown restrictions on BC mass concentrations and submicron aerosol mass concentrations were assessed at the high-altitude site HACPL, Mahabaleshwar in western India, during the pre-lockdown (1st February to 20th March) and lockdown period (28th March to 31st May) of 2020 using the dual-spot multi-wavelength aethalometer (AE-33) and HR-TOF AMS. The characteristics of BC during pre-lockdown and lockdown, with a focus on its source apportionment, were thoroughly studied and compared with similar periods in previous years (2017 and 2018). BC concentration was 44% lower during the lockdown period in 2020 than during the pre-lockdown period 2020. The shape of its diurnal variation changed with a considerable decrease in sharp morning and evening peaks. Comparing BC concentration during the lockdown period of 2020 with a similar period in previous years (2017 and 2018) revealed that the BC concentration did not decrease substantially because of the lockdown. Submicron organics also indicated similar variability, supporting this conclusion. The lower decrease in BC concentration at Mahabaleshwar than at other locations in India could be partially attributed to the enhanced BC from biomass burning during the lockdown. The source apportionment of BC also revealed that BC emissions from biomass burning sources increased significantly (50% of total BC) during the lockdown period of 2020, while higher emissions (80%) from traffic or fossil fuel during the pre-lockdown period of 2020 were noticed. BrC contributed 26% to the total absorption at 370 nm during the lockdown period, higher than similar periods in 2017 and 2018. This observation indicated a significant abundance of BrC during the lockdown period due to biomass burning sources. Radiative forcing due to BC was also evaluated during both periods. The estimated atmospheric radiative forcing decreased from March to May 2020 (lockdown period). However, a comparison of atmospheric radiative forcing during the lockdown period with the previous years (2017 and 2018) revealed that the BC radiative forcing decreased by 8% during the lockdown period in 2020.

Although many studies have indicated a significant decrease in aerosol loading and black carbon concentration over many regions during the COVID-19 lockdown in 2020, our study contradicts these findings to some extent. This study revealed that heterogeneity in different sources may result in varying impacts on atmospheric BC abundance. Furthermore, this study also ascertains the importance of biomass burning in the Western Ghats region, especially in the absence of other anthropogenic activities during the lockdown period. The BrC co-emitted from biomass burning also affects the radiation budget. Hence, the radiative forcing estimated here (with BC only) may be underestimated considering the large contribution from biomass burning to emitted BC. Further studies are required to estimate the radiative impact of BrC over this region.

Declaration of competing interest

The authors declare that they have no known competing financial interests or personal relationships that could have appeared to influence the work reported in this paper.

Acknowledgments

The authors are thankful to the Director, IITM for his continuous encouragement and support. IITM is fully funded by the Ministry of Earth sciences, Govt. of India. Authors are also thankful to Mr. Avishek Roy, IITM, Pune for help with the 2020 HR-TOF AMS data.

Appendix A. Supplementary data

Supplementary data to this article can be found online at https://doi.org/10.1016/j.apr.2022.101566.

References

Aiken, A.C., Decarlo, P.F., Kroll, J.H., Worsnop, D.R., Huffman, J.A., Docherty, K.S., Ulbrich, I.M., Mohr, C., Kimmel, J.R., Sueper, D., Sun, Y., Zhang, Q., Trimborn, A., Northway, M., Ziemann, P.J., Canagratna, M.R., Onasch, T.B., Alfarra, M.R., Prevot, A.S.H., Dommen, J., Duplissy, J., Metzger, A., Baltensperger, U.R.S., Jimnez, J., 2008. O/C and OM/OC ratios of primary, secondary, and ambient organic aerosols with high-resolution time-of-flight aerosol mass spectrometry. Environ. Sci. Technol. 42 (12), 4478–4485.

Ajay, A., Krishna Moorthy, K., Satheesh, S.K., Ilavazhagan, G., 2021. Impact of lockdown-related reduction in anthropogenic emissions on aerosol characteristics in the megacity. Bengaluru. Curr. Sci. 120 (2), 287–295.

Alfarra, M.R., Prévôt, A.S.H., Szidat, S., Sandradewi, J., Weimer, S., Lanz, V.A., Schreiber, D., Mohr, M., Baltensperger, U., 2007. Identification of the massspectral signature of organic aerosols from woodburning emissions. Environ. Sci. Technol. 41, 5770–5777.

Andreae, M.O., Gelencs, A., Box, P.O., Veszpr, H., 2006. Black carbon or brown carbon? The nature of light-absorbing carbonaceous aerosols. Atmos. Chem. Phys. 6, 3131–3148. https://acp.copernicus.org/articles/6/3131/2006/acp-6-3131-2006.pdf.

Bhawar, R.L., Fadnavis, S., Kumar, V., Rahul, P.R.C., Sinha, T., Lolli, S., 2021. Radiative impacts of aerosols during COVID-19 lockdown period over the Indian region. Front. Environ. Sci. 9, 746090 https://doi.org/10.3389/fenvs.2021.746090.

Bond, T.C., Doherty, S.J., Fahey, D.W., Forster, P.M., Berntsen, T., Deangelo, B.J., Flanner, M.G., Ghan, S., Kärcher, B., Koch, D., Kinne, S., Kondo, Y., Quinn, P.K., Sarofim, M.C., Schultz, M.G., Schulz, M., Venkataraman, C., Zhang, H., Zhang, S., Bellouin, N., Guttikunda, S.K., Hopke, P.K., Jacobson, M.Z., Kaiser, J.W., Klimont, Z., Lohmann, U., Schwarz, J.P., Shindell, D., Storelvmo, T., Warren, S.G., Zender, C.S., 2013. Bounding the role of black carbon in the climate system: a scientific assessment. J. Geophys. Res. Atmos. 118, 5380–5552. https://doi.org/10.1002/jgrd.50171.

Buchunde, P.S., Safai, P.D., Mukherjee, S., Raju, M.P., Meena, G.S., Sonbawne, S.M., Dani, K.K., Pandithurai, G., 2022. Seasonal abundances of primary and secondary carbonaceous aerosols at a high-altitude station in the Western Ghat Mountains, India. Air. Qual. Atmos. Health 15, 209–220. https://doi.org/10.1007/s11869-021-01097-5.

Cape, J.N., Coyle, M., Dumitrean, P., 2012. The atmospheric lifetime of black carbon. Atmos. Environ. 59, 256–263.

Chakrabarty, R.K., Moosmüller, H., Chen, L.W., Lewis, K., Arnott, W.P., Mazzoleni, C., Dubey, M.K., Wold, C.E., Hao, W.M., Kreidenweis, S.M., 2010. Brown carbon in tar balls from smoldering biomass combustion. Atmos. Chem. Phys. 10, 6363–6370.

Chen, Y., Bond, T.C., 2010. Light absorption by organic carbon from wood combustion. Atmos. Chem. Phys. 10, 1773–1787. https://doi.org/10.5194/acp-10-1773-2010.

Collaud, Coen M., Weingartner, E., Apituley, A., Ceburnis, D., Fierz-Schmidhauser, R., Flentje, H., Henzing, J.S., Jennings, S.G., Moerman, M., Petzold, A., Schmid, O., Baltensperger, U., 2010. Minimizing light absorption measurement artifacts of the Aethalometer: evaluation of five correction algorithms. Atmos. Meas. Tech. 3 (2), 457–474.

Crippa, M., DeCarlo, P.F., Slowik, J.G., Mohr, C., Heringa, M.F., Chirico, R., Poulain, L., Freutel, F., Sciare, J., Cozic, J., Di Marco, C.F., 2013. Winter time aerosol chemical composition and source apportionment of the organic fraction in the metropolitan area of Paris. Atmos. Chem. Phys. 13, 961–981.

Draxler, R.R., Rolph, G.D., 2003. HYSPLIT (Hybrid Single-Particle Lagrangian Integrated Trajectory) Model Access via NOAA ARL READY NOAA Air Resources Laboratory. Silver Spring. http://ready.arl.noaa.gov/HYSPLIT.php.

Drinovec, L., Mocnik, G., Zotter, P., Prévôt, A.S.H., Ruck-stuhl, C., Coz, E., Rupakheti, M., Sciare, J., Müller, T., Wieden-sohler, A., Hansen, A.D.A., 2015. The "dual-spot" Aethalometer: an improved measurement of aerosol black carbon with real time loading compensation. Atmos. Meas. Tech. 8, 1965–1979. https://doi.org/10.5194/amt-8-1965-2015.

Dumka, U.C., Kaskaoutis, D.G., Tiwari, S., Safai, P.D., Attri, S.D., Soni, V.K., Singh, N., Mihalopoulos, N., 2018. Assessment of biomass burning and fossil fuel contribution to black carbon concentrations in Delhi during winter. Atmos. Environ. 194, 93–109.

Feng, Y., Ramanathan, V., Kotamarthi, V.R., 2013. Brown carbon: a significant atmospheric absorber of solar radiation? Atmos. Chem. Phys. 13 (17), 8607–8621.

Formenti, P., Elbert, W., Maenhaut, W., Haywood, J., Osborne, S., Andreae, M.O., 2003. Inorganic and carbonaceous aerosols during the Southern African Regional Science Initiative (SAFARI 2000) experiment: chemical characteristics, physical properties, and emission data or smoke from African biomass burning. J. Geophys. Res. Atmos. 108 (13), 1–16. https://doi.org/10.1029/2002jd002408.

Goel, V., Hazarika, N., Kumar, M., Singh, V., Thamban, N.M., Tripathi, S.N., 2021. Variations in Black Carbon concentration and sources during COVID19 lockdown in Delhi. Chemosphere 270, 129435. https://doi.org/10.1016/j.chemosphere.2020.129435.

Gysel, M., Laborde, M., Olfert, J.S., Subramanian, R., Grohn, A.J., 2011. Effective density of Aquadag and fullerene soot black carbon reference materials used for SP2 calibration. Atmos. Meas. Tech. 4 (12), 2851–2858.

Hansen, A.D.A., Rosen, H., Novakov, T., 1984. The aethalometer: an instrument for the real time measurements of optical absorption by aerosol particles. Sci. Total Environ. 36.

Hansen, A.D.A., 2007. Operating Manual for the AE31/22/42 Aethalometers. Magee Scientific, Berkeley, pp. 191–196. California.

Harrison, R.M., Beddows, D.C., Jones, A.M., Calvo, A., Alves, C., Pio, C., 2013. An evaluation of some issues regarding the use of aethalometers to measure woodsmoke concentrations. Atmos. Environ. 80, 540–548.

Healy, R.M., Wang, J.M., Jeong, C.H., Lee, A.K., Willis, M.D., Jaroudi, E., Zimmerman, N., Hilker, N., Murphy, M., Eckhardt, S., Stohl, A., 2015. Light-absorbing properties of ambient black carbon and brown carbon from fossil fuel and biomass burning sources. J. Geophys. Res. Atmos. 120 (13), 6619–6633.

Hess, M., Koepke, P., Schult, I., 1998. Optical properties of aerosols and clouds: the software package OPAC. Bull. Am. Meteorol. Soc. 79, 831–844.

Hoffer, A., Gelencsér, A., Guyon, P., Kiss, G., Schmid, O., Frank, G.P., Artaxo, P., Andreae, M.O., 2006. Optical properties of humiclike substances (HULIS) in biomass-burning aerosols. Atmos. Chem. Phys. 6, 3563–3570. https://doi.org/10.5194/acp-6-3563- 2006.

Jafar, H.A., Harrison, R.M., 2020. Spatial and temporal trends in carbonaceous aerosols in the United Kingdom. Atmos. Pollut. Res. 12 (1), 295–305. https://doi.org/10.1016/j.apr.2020.09.009.

Janssen, A.H., Gerlofs-Nijland, M.E., Lanki, T., Salonen, R.O., Cassee, F., Hoek, G., Fischer, P., Brunekreef, B., Krzyzanowski, M., 2012. Health Effects of Black Carbon. WHO. https://www.euro.who.int/_data/assets/pdf_file/0004/162535/e96541.pdf.

Kirchstetter, T.W., Novakov, T., Hobbs, P.V., 2004. Evidence that the spectral dependence of light absorption by aerosols is affected by organic carbon. J. Geophys. Res. Atmos. 109 (21), 1–12. https://doi.org/10.1029/2004JD004999.

Kodandapani, N., 2013. Contrasting fire regimes in a seasonally dry tropical forest and a savanna ecosystem in the Western Ghats, India. Fire Ecology 9 (2), 102–115.

Lack, D.A., Cappa, C.D., 2010. Impact of brown and clear carbon on light absorption enhancement, single scatter albedo and absorption wavelength dependence of black carbon. Atmos. Chem. Phys. 10, 4207–4220.

Lack, D.A., Langridge, J.M., 2013. On the attribution of black and brown carbon light absorption using the Ångström exponent. Atmos. Chem. Phys. 13 (20), 10535–10543.

Lack, D.A., Langridge, J.M., Bahreini, R., Cappa, C.D., Middlebrook, A.M., Schwarz, J.P., 2012. Brown carbon and internal mixing in biomass burning particles. Proc. Natl. Acad. Sci. U. S. A 109 (37), 14802–14807.

Lack, D.A., Bahreini, R., Langridge, J.M., Gilman, J.B., Middlebrook, A.M., 2013. Brown carbon absorption linked to organic mass tracers in biomass burning particles. Atmos. Chem. Phys. 13, 2415–2422. https://doi.org/10.5194/acp-13-2415-2013.

Laskin, A., Laskin, J., Nizkorodov, S.A., 2015. Chemistry ofAtmospheric Brown carbon. Chem. Rev. 115 (10), 4335–4382.

Lewis, K., Arnott, W.P., Moosmüller, H., Wold, C.E., 2008. Strong spectral variation of biomass smoke light absorption and single scattering albedo observed with a novel dual-wavelength photoacoustic instrument. J. Geophys. Res. Atmos. 113, D16203 https://doi.org/10.1029/2007JD009699.

Lund, M.T., Samset, B.H., Skeie, R.B., Watson-Parris, D., Katich, J.M., Schwarz, J.P., Weinzierl, B., 2018. Short Black Carbon lifetime inferred from a global set of aircraft observations. Npj Climate and Atmos. Sci. 1 (1), 1–8.

Manohar, M., Atanacio, A., Button, D., Cohen, D., 2021. MABI—a multi-wavelength absorption black carbon instrument for the measurement of fine light absorbing carbon particles. Atmos. Pollut. Res. 12, 133–140.

Marinoni, A., Cristofanelli, P., Laj, P., Duchi, R., Calzolari, F., Decesari, S., Sellegri, K., Vuillermoz, E., Verza, G.P., Villani, P., Bonasoni, P., 2010. Aerosol mass and black carbon concentrations, a two year record at NCO-P (5079 m, Southern Himalayas). Atmos. Chem. Phys. 10 (17), 8551–8562.

Meena, G.S., Mukherjee, S., Buchunde, P., Safai, P.D., Singla, V., Aslam, M.Y., Sonbawne, S.M., Made, R., Anand, V., Dani, K.K., Pandithurai, G., 2021. Seasonal variability and source apportionment of black carbon over a rural high-altitude and an urban site in western India. Atmos. Pollut. Res. 12, 32–45. https://doi.org/10.1016/j.apr.2020.10.006.

Milinković, A., Gregorič, A., Grgičin, V.D., Vidič, S., Penezić, A., Kušan, A.K., Alempijević, S.B., Kasper-Giebl, A., Frka, S., 2021. Variability of black carbon aerosol concentrations and sources at a Mediterranean coastal region. Atmos. Pollut. Res. 12, 101221 https://doi.org/10.1016/j.apr.2021.101221.

Mohr, C., Lopez-Hilfiker, F.D., Zotter, P., Prévot, A.S., Xu, L., Ng, N.L., Herndon, S.C., Williams, L.R., Franklin, J.P., Zahniser, M.S., Worsnop, D.R., 2013. Contribution of nitrated phenols to wood burning brown carbon light absorption in Detling, United Kingdom during winter time. Environ. Sci. Technol. 47 (12), 6316–6324.

Mukherjee, S., Singla, V., Pandithurai, G., Safai, P.D., Meena, G.S., Dani, K.K., 2018. Seasonal variability in chemical composition and source apportionment of sub-micron aerosol over a high altitude site in Western Ghats, India. Atmos. Environ. 180, 79–92. https://doi.org/10.1016/j.atmosenv.2018.02.048.

Mukherjee, S., Singla, V., Meena, G.S., Aslam, M.Y., Safai, P.D., Buchunde, P., Vasudevan, A.K., Jena, C.K., Ghude, S.D., Dani, K., Pandithurai, G., 2020. Submicron aerosol variability and its ageing process at a high altitude site in India: impact of meteorological conditions. Environ. Pollut. 265, 115019 https://doi.org/10.1016/j.envpol.2020.115019.

Mukherjee, S., Anil Kumar, V., Patil, R.D., Meena, G.S., Buchunde, P., Waghmare, V., Deshmukh, S., Dhavale, V., Ray, A., Panicker, A.S., Sonbawne, S.M., Safai, P.D., Pandithurai, G., 2021. Investigation of physico-chemical characteristics and associated CCN activation for different combustion sources through Chamber experiment approach. Atmos. Environ. 266, 1–9. https://doi.org/10.1016/j.atmosenv.2021.118726.

Ng, N.L., Canagaratna, M.R., Jimenez, J.L., Chhabra, P.S., Seinfeld, J.H., Worsnop, D.R., 2011. Changes in organic aerosol composition with aging inferred from aerosol mass spectra. Atmos. Chem. Phys. 11, 6465–6474. https://doi.org/10.5194/acp-11-6465-2011.

Palle, S.N.R., Tandule, C.R., Kalluri, R.O.R., Gugamsetty, B., Kotalo, R.G., Thotli, L.R., Akkiraju, B., Lingala, S.S.R., 2021. The impact of lockdown on eBC mass concentration over a semi-arid region in southern India: ground observation and model simulations. Aerosol Air Qual. Res. 21, 210101 https://doi.org/10.4209/aaqr.210101.

Pandey, S.K., Vinoj, V., 2021. Surprising changes in aerosol loading over India amid covid-19 lockdown. Aerosol Air Qual. Res. 21, 200466 https://doi.org/10.4209/aaqr.2020.07.0466.

Panicker, A.S., Pandithurai, G., Safai, P.D., Dipu, S., Lee, D.I., 2010. On the contribution of black carbon to the composite aerosol radiative forcing over an urban environment. Atmos. Environ. 44, 3066–3070.

Panicker, A.S., Park, S.H., Lee, D.I., Kim, D.C., Jung, W.S., Jang, S.M., Jeong, J.H., Kim, D.S., Yu, D.S., Yu, J., Jeong, H., 2013. Observations of black carbon characteristics and radiative forcing over a global atmosphere watch supersite in Korea. Atmos. Environ. 77, 98–104. https://doi.org/10.1016/j.atmosenv.2013.04.020.

Petit, J.E., Favez, O., Albinet, A., Canonaco, F., 2017. A user-friendly tool for comprehensive evaluation of the geographical origins of atmospheric pollution: wind and trajectory analyses. Environ. Model. Software 88, 183–187.

Rajesh, T.A., Ramachandran, S., 2022. Assessment of the coronavirus disease 2019 (COVID-19) pandemic imposed lockdown and unlock effects on black carbon aerosol, its source apportionment, and aerosol radiative forcing over an urban city in India. Atmos. Res. 267, 105924.

Raju, M.P., Safai, P.D., Rao, P.S.P., Devara, P.C.S., Budhavant, K.B., 2011. Seasonal characteristics of black carbon aerosols over a high altitude station in Southwest India. Atmos. Res. 100, 103–110. https://doi.org/10.1016/j.atmosres.2011.01.006.

Raju, M.P., Safai, P.D., Vijayakumar, K., Devara, P.C.S., Naidu, C.V., Rao, P.S.P., Pandithurai, G., 2016. Atmospheric abundances of black carbon aerosols and their radiative impact over an urban and a rural site in SW India. Atmos. Environ. 125, 429–436. https://doi.org/10.1016/j.atmosenv.2015.09.023.

Rathod, T.D., Sahu, S.K., Tiwari, M., Bhangare, R.C., Ajma, P.Y., 2021. Light absorption enhancement due to mixing in black carbon and organic carbon generated during biomass burning. Atmos. Pollut. Res. 12, 101236 https://doi.org/10.1016/j.apr.2021.101236.

Ratnam, V., Prasad, P., Raj, S.A., Ibrahim, H., 2021. Effect of lockdown due to COVID-19 on the aerosol and trace gases spatial distribution over India and adjoining regions. Aerosol Air Qual. Res. 21, 200397.

Reyes-Villegas, E., Panda, U., Darbyshire, E., Cash, J.M., Joshi, R., Langford, B., Marco, C.F. Di, Mullinger, N.J., Alam, M.S., Crilley, L.R., Rooney, D.J., Acton, W.J.F., Drysdale, W., Nemitz, E., Flynn, M., Voliotis, A., Mcfiggans, G., Coe, H., Lee, J., Hewitt Heal, M.R., Gunthe, S.S., Mandal, T.K., Gurjar, B.R., Shivani Gadi, R., Singh, S., Soni, V., Allan, J.D., 2021. PM_1 composition and source apportionment at two sites in Delhi , India , across multiple seasons. Atmos. Chem. Phys. 21, 11655–11667.

Ricchiazzi, P., Yang, S., Gautier, C., Sowle, D., 1998. SBDART, A research and teaching tool for plane-parallel radiative transfer in the Earth's atmosphere. Bull. Am. Meteorol. Soc. 79, 2101–2114.

Russell, P.B., Bergstrom, R.W., Shinozuka, Y., Clarke, A.D., Decarlo, P.F., Jimenez, J.L., Livingston, J.M., 2010. Absorption Angstrom Exponent in AERONET and related data as an indicator of aerosol composition. Atmos. Chem. Phys. 10, 1155–1169. https://doi.org/10.5194/acp-10-1155-2010.

Safai, P.D., Devara, P.C.S., Raju, M.P., Vijayakumar, K., Rao, P.S.P., 2014. Relationship between black carbon and associated optical, physical and radiative properties of aerosols over two contrasting environments. Atmos. Res. 149, 292–299. https://doi.org/10.1016/j.atmosres.2014.07.006.

Saleh, R., Robinson, E.S., T kacik, D., Ahern, A.T., Liu, S., Aiken, A.C., Sullivan, R.C., Presto, A.A., Dubey, M.K., Yokelson, R.J., Donahue, N.M., Robinson, A.L., 2014. Brownness of organics in aerosols from biomass burninglinked to their black carbon content. Nat. Geosci. 7, 647–650. https://doi.org/10.1038/NGEO2220.

Sandradewi, J., Prévôt, A.S.H., Szidat, S., Perron, N., Alfarra, M.R., Lanz, V.A., Weingartner, E., Baltensperger, U., 2008. Using aerosol light absorption measurements for the quantitative determination of wood burning and traffic emission contributions to particulate matter. Environ. Sci. Technol. 42, 3316–3323. https://doi.org/10.1021/es702253m.

Schwarz, J.P., Gao, R.S., Fahey, D.W., Thomson, D.S., Watts, L.A., Wilson, J.C., Reeves, J. M., Darbeheshti, M., Baumgardner, D.G., Kok, G.L., Chung, S.H., 2006. Single-particle measurements of midlatitude black carbon and light-scattering aerosols from the boundary layer to the lower stratosphere. J. Geophys. Res. Atmos. 111 (D16).

Schwarz, J.P., Spackman, J.R., Gao, R.S., Perring, A.E., Cross, E., Onasch, T.B., Ahern, A., Wrobel, W., Davidovits, P., Olfert, J., Dubey, M.K., 2010. The detection efficiency of the single particle soot photometer. Aerosol Sci. Technol. 44 (8), 612–628.

Shen, Z., Ming, Y., Horowitz, L.W., Ramaswamy, V., Lin, M., 2017. On the seasonality of Arctic black carbon. J. Clim. 30 (12), 4429–4441.

Shen, L., Wang, H., Kong, X., Zhang, C., Shi, S., Zhu, B., 2021. Characterization of black carbon aerosol in the Yangtze River Delta, China: seasonal variation and source apportionment. Atmos. Pollut. Res. 12, 195–209.

Singh, P., Sarawade, P., Adhikary, B., 2020. Transport of black carbon from planetary boundary layer to free troposphere during the summer monsoon over South Asia. Atmos. Res. 235, 104761.

Singla, V., Mukherjee, S., Kashikar, A.S., Safai, P.D., Pandithurai, G., 2018. Black carbon : source apportionment and its implications on CCN activity over a rural region in Western Ghats , India. Environ. Sci. Pollut. Res. 26, 7071–7081.

Srivastava, R., Ramachandran, S., Rajesh, T.A., Kedia, S., 2011. Aerosol radiative forcing deduced from observations and models over an urban location and sensitivity to single scattering albedo. Atmos. Environ. 45, 6163–6171.

Twomey, S., 1977. The influence of pollution on the shortwave albedo of clouds. J. Atmos. Sci. 34, 1149–1152.

Virkkula, A., Mäkelä, T., Yli-Tuomi, T., Hirsikko, A., Koponen, I.K., Hämeri, K., Hillamo, R., 2007. A simple procedure for correcting loading effects of aethalometer data. J. Air Waste Manage. 57, 1214–1222.

Wang, J., Nie, W., Cheng, Y., Shen, Y., Chi, X., Wang, J., Huang, X., Xie, Y., Sun, P., Xu, Z., Qi, X., Su, H., Ding, A., 2018. Light absorption of brown carbon in eastern China based on 3-year multi-wavelength aerosol optical property observations and an improved absorption Ångström exponent segregation method. Atmos. Chem. Phys. 18, 9061–9074. https://doi.org/10.5194/acp-18-9061-2018.

Wang, Y., Hopke, P.K., Utell, M.J., 2011. Urban-scale spatial-temporal variability of black carbon and winter residential wood combustion particles. Aerosol Air Qual. Res. 11, 473–481. https://doi.org/10.4209/aaqr.2011.01.0005.

Wang, Y., Hopke, P.K., Xia, X., Rattigan, O.V., Chalupa, D.C., Utell, M.J., 2012. Source apportionment of airborne particulate matter using inorganic and organic species as tracers. Atmos. Environ. 55, 525–532.

Wang, P., Wang, H., Wang, Y., Zhang, X.Y., Gong, S.L., Xue, M., Zhou, C.H., Liu, H.L., An, X.Q., Niu, T., Cheng, Y.L., 2016. Inverse modelling of black carbon emissions over China using ensemble data assimilation. Atmos. Chem. Phys. 16, 989–1002. https://doi.org/10.5194/acp-16-989-2016.